In: Gendt, G., Dick, G. (Ed.): Special Topics and New Directions., Proc. of the 1995 IGS Workshop, Potsdam, pp 57-66.

MONITORING IONOSPHERIC DISTURBANCES USING THE IGS NETWORK

Lambert Wanninger
Geodetic Institute, TU Dresden
D-01062 Dresden
Germany

ABSTRACT

Small-scale ionospheric irregularities disturb GPS signals in two ways: they produce fluctuations in signal strength (amplitude scintillations) and rapid changes in ionospheric delay (phase scintillations). GPS observation data provided by the IGS network are an excellent resource for monitoring phase scintillation occurrence. Examples of phase scintillation occurrence maps produced from IGS data demonstrate their importance not only for ionospheric research but also for GPS users.

INTRODUCTION

The ionosphere is well known by GPS users as a source of refraction errors which can effectively be corrected by simultaneous dual-frequency observations. The highest total ionospheric electron contents (TEC) and thus the largest ionospheric refraction delays are found in the equatorial region (Fig. 1, Fig. 3). They not only cause single-frequency coordinate errors but also difficulties in single-frequency and dual-frequency carrier phase ambiguity resolution. In relative positioning, large-scale gradients of the vertical TEC often produce larger errors than absolute TEC.

This paper, however, deals with the effects of the disturbed ionosphere on GPS signals and GPS positioning. It concentrates on small-scale irregularities in the electron density which cause signal scintillation. Since the early days of GPS it has been known that signal scintillation is by far the most serious problem in transionospheric propagation (*Parkinson et al. 1977*). Scintillation degrades GPS receiver performance: an increased number of cycle slips and even the inability to track the GPS signals (data loss) can occur. The effects of ionospheric scintillation on GPS

	IONOSPHERE			
	undisturbed		disturbed	
	constant vertical TEC	large-scale gradient	small-scale: scintillation	medium-scale: MSTID ...
region mainly affected	equatorial region	equatorial region	equatorial, polar regions	mid-latitudes, ...
effects on GPS	L_1-coordinate errors, difficulties in ambiguity resolution	L_1-coordinate errors, difficulties in ambiguity resolution even for short baselines	degrades receiver performance → data loss, cycle slips; difficulties to fix cycle slips	L_1-coordinate errors, difficulties in ambiguity resolution for short observation periods ($\leq$ 20 min)
what IGS can contribute	global TEC-models	global TEC-models, + regional models with higher resolution	scintillation occurrence maps	TID occurrence maps
long-term objectives	improved correction models		prediction of occurrence	

Fig. 1: GPS, IGS, and the ionosphere.

signals can be detected in GPS observations and thus the geographical and temporal occurrence of small-scale ionospheric irregularities can be monitored.

SCINTILLATION EFFECTS ON GPS

Severest effects of small-scale ionospheric irregularities are signal fading and signal enhancement, collectively known as amplitude scintillations. As a result of these scintillations, the level of a GPS signal can drop below a receiver's lock threshold. This threshold depends on the bandwidth of the GPS receiver system and on the type of tracking channel. Amplitude scintillations can be monitored by interpretation of time series of S/N values provided by many GPS receivers. Rapidly changing values indicate scintillation activity (Fig. 2). Missing S/N values for the disturbed satellite pass indicate that the receiver could not continuously track the GPS signal. Data loss and an increased number of cycle slips are a consequence of this scintillation activity.

Phase scintillations result from sudden changes in ionospheric refraction or from diffraction effects. Because of these scintillations, the phase of both the L_1 and L_2 carriers can change by several cycles between two measurements spaced by, for

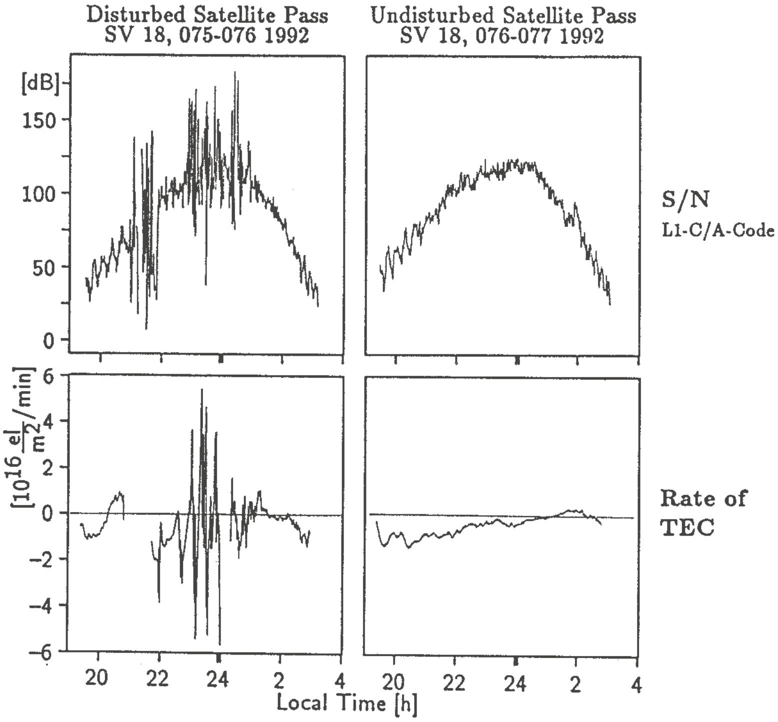

Fig. 2: Effects of equatorial scintillations on GPS measurements from southern Brazil: amplitude scintillations, phase scintillations (*Wanninger 1993b*).

example, 30 seconds. Such perturbations complicate cycle slip detection and repair. They can easily be detected in continuous dual-frequency phase data. The lower two panels of Figure 2 show the change of ionospheric refraction from one minute to the next as derived from dual-frequency phase data. Missing values for the disturbed satellite pass show that no continuous dual-frequency phase data were available for a considerable time period.

The scintillation effects shown in Figure 2 belong to the worst effects to be expected for GPS signals. They were observed in Curitiba (Brazil) in March of 1992, thus few degrees south of the magnetic equator during an equinox month and in a year of high solar activity. Most probably no such severe effects have disturbed any IGS data till today. In 1995, with some IGS stations close to the magnetic equator (Arequipa, Fortaleza, Bangalore), solar activity is at its minimum level and thus such severe effects are not expected. But in 1992, with a higher level of solar activity, no IGS stations existed in the center of the equatorial region. With the advent of the next period of high solar activity around the end of this decade, those effects will be observable at many equatorial IGS stations.

OCCURRENCE OF SMALL-SCALE DISTURBANCES

The region of equatorial scintillations extends 30° on either side of the earth's magnetic equator (Fig. 3). The strongest effects are found at approximately 10° N and

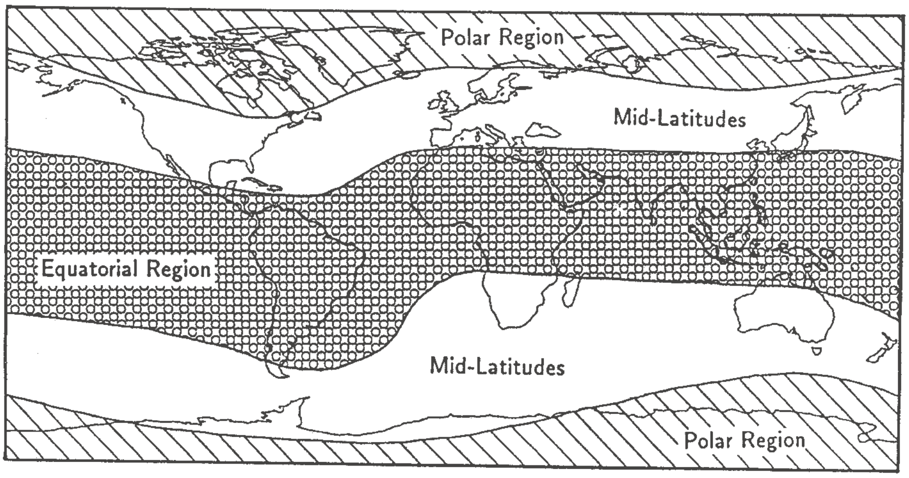

Fig. 3: Ionospheric regions of the world.

S. There is a clear diurnal variation: scintillations occur between approximately one hour after sunset and midnight and occasionally continue until dawn. In addition, there is a seasonal dependence: strongest effects are found in equinox months. A high level of occurrence is observed between September and April in the longitude band stretching from the Americas to Africa. In the Indian and Pacific region, however, a high level of occurrence is found between March and October (*Basu et al. 1988, Aarons 1993*).

Polar scintillations are not as strong as those near the equator. Their occurrence is closely related to magnetic storm activity. The strongest ionospheric activity does not take place in the polar cap regions but rather in the auroral zones situated at the boundary of polar regions and mid-latitudes between magnetic latitudes of about 64° and about 70°. During strong magnetic storms, these auroral effects can extend well into the mid-latitudes. The equatorward extension of polar scintillation activity is of primary interest to GPS users in the mid-latitudes.

Furthermore, scintillation effects depend on the 11-year solar cycle. Their level of occurrence and their intensity increase with an increase in the solar sunspot numbers. From 1989 to 1992, they were especially strong due to the maximum of solar cycle No. 22. From 1994 to 1997, minimal occurrence and minimal strength can be expected. But around the year 2000, scintillation effects will increase again.

GPS SCINTILLATION MONITORING

Amplitude scintillations can be detected in time series of S/N values provided by many GPS receivers. Unfortunately, when raw data (in a binary receiver dependent format) are converted to RINEX format, most of the S/N information gets lost as the S/N values are projected onto the interval 1 to 9. Since all IGS observations are available in RINEX format only, no use can be made of this valuable information of the GPS signal strength.

Phase scintillations can easily be detected in continuous dual-frequency GPS phase observations. The vast amount of such data in the IGS archives presents an important resource for research on ionospheric phase scintillations.

Other desirable features for scintillation monitoring are the ability to record phase (and amplitude) observations at a rate of at least 1 Hz and with a tracking loop bandwidth of some Hz. These characteristics are needed to investigate the structure and dynamics of small-scale irregularities. These features, however, do not exist for the IGS data (30 seconds recording rate, small tracking loop bandwidth).

In summary, the IGS network does not provide ideal GPS observations for scintillation monitoring, but the dual-frequency phase data can be used for phase scintillation detection and can therefore give indications of the geographical and temporal occurrence of small-scale irregularities.

DETECTION OF PHASE SCINTILLATION IN IGS DATA

Phase scintillations can easily be detected in the time-differenced ionospheric ("geometry-free") linear combination of single-station dual-frequency phase observations. This unambiguous observable provides the rate of change of ionospheric delay, which is converted to the rate of change of the total ionospheric electron content (Rate of TEC – RoT $[10^{16} m^{-2} min^{-1}]$):

$$RoT = 9.52 \cdot ((\Phi_1 - \Phi_2)_{tj} - (\Phi_1 - \Phi_2)_{ti}) \tag{1}$$

with

$$\Delta t = t_j - t_i = 1 \ min. \tag{2}$$

Φ_1 and Φ_2 [m] are the measured carrier beat phase observables of L_1 and L_2 respectively, t_i and t_j are the measurement epochs, the scaling factor converts the ionospheric delay difference to units of $[electrons/m^2]$ (*Wanninger 1993a*).

All frequency independent errors are removed by forming the ionospheric linear combination. Significant remaining errors are multipath, which can reach up to $0.3 \cdot 10^{16} m^{-2} min^{-1}$, and random observation errors, which usually do not exceed $0.07 \cdot 10^{16} m^{-2} min^{-1}$. Cycle slips have to be detected in the pre-processing. They do not need to be estimated, but time-differencing is performed for continuous observations only. Similar observables are found in several publications or software-packages (e.g. *Wild et al. 1989, UNAVCO 1994, Doherty et al. 1994*). They mainly differ in respect to epoch rate and units. Their information content concerning phase scintillations is identical.

The RoT-values of complete satellite passes and various ionospheric conditions are shown in Figure 4. They illustrate (from left to right) undisturbed ionospheric conditions, polar scintillations, equatorial scintillations, and equatorial scintillations with receiver tracking difficulties causing data gaps. Low frequency spectral components are caused by vertical TEC and by large-scale gradients of vertical TEC.

In order to simplify scintillation detection, a phase scintillation index I_{GPS} is computed from RoT values. In a first processing step, the RoT time series are high

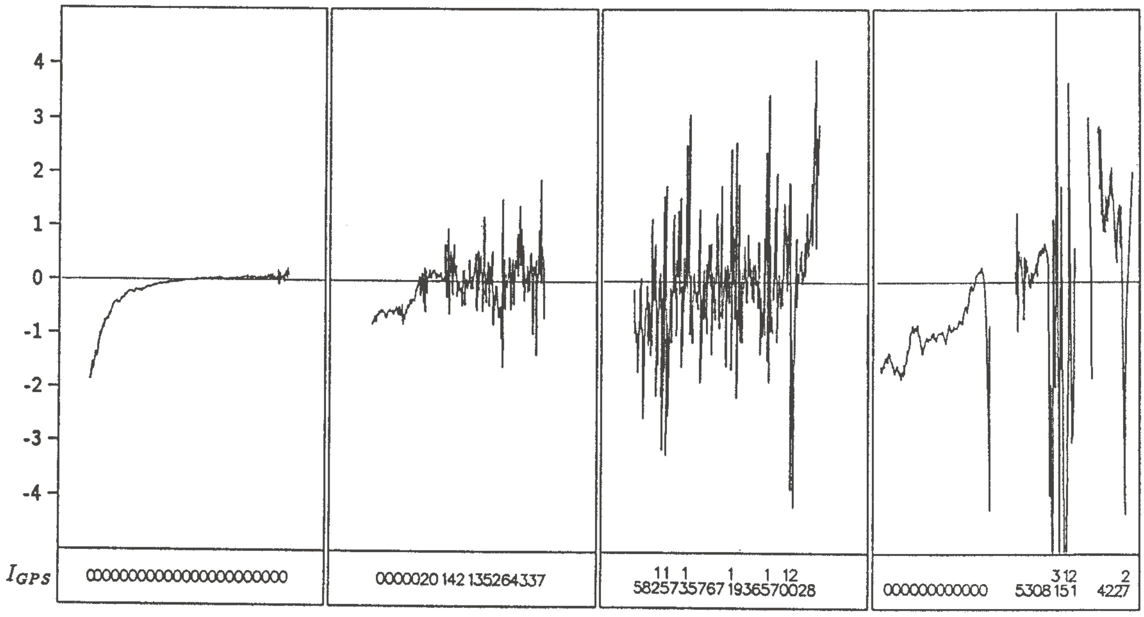

Fig. 4: Rate of change of TEC (RoT in $[10^{16} m^{-2} min^{-1}]$) and phase scintillation index I_{GPS}.

pass filtered in order to remove low frequency components. The index is computed as RMS over n epochs of the remaining components of RoT time series ($\overline{RoT}$):

$$I_{GPS} = 10 \cdot \sqrt{\frac{1}{n} \sum_{epochs} \overline{RoT}^2}. \tag{3}$$

Examples of I_{GPS} values of 15 minute blocks of observations are presented in Fig. 4. Other kinds of index definitions should also be considered and should be tested against this RMS-type index.

It is expected that small-scale irregularities in the electron content cause larger phase scintillations for signals coming from satellites at low elevation compared with scintillations for signals arriving from zenith direction. However, such an elevation dependence could not be confirmed with actual GPS observations. Thus, no reduction of I_{GPS} values to zenith direction is performed. Further investigations on the elevation dependence of GPS phase scintillations are needed.

In a last processing step spatial information is assigned to every index value. Having just one observation site, it is sufficient to use the satellite's azimuth and elevation which provide the direction to the area sampled. However, in order to combine index values of several sites, sub-ionospheric coordinates have to be computed. They consist of latitude and longitude (or local time) of the intersection points of the GPS signals with an ionospheric shell in a certain height above the earth surface. Since the actual height of small-scale irregularities, which could be as low as 250 km or as high as 600 km, is usually not known, an average height (400 km) is taken for coordinate computations. The examples presented below were computed with this ionospheric height.

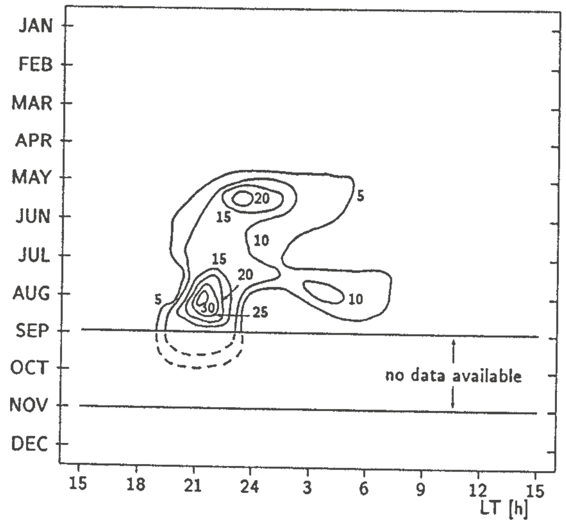

Fig. 5:
Percentage occurrence of phase scintillations at Kokee Park, Hawaii 1992: $I_{RoT} \geq 3$ in periods of 30 minutes, elevation mask 15°, mid-month marked, local time of sub-ionospheric points (400 km).

Example 1: Kokee Park, Hawaii 1992

Hawaii is located at 20°N magnetic latitude. It belongs to the ionospheric equatorial region. Though the main scintillation activity takes place around ±10° magnetic latitude, Hawaii is also expected to be affected. Of major interest is the temporal (seasonal, diurnal) distribution of the disturbances.

Kokee Park data are available for the whole of 1992, with the exception of a data gap from mid-September to mid-November. Figure 5 shows the percentage occurrence of phase scintillations as derived from phase scintillation index values I_{GPS} (*Wanninger 1993a*).

No scintillation occurrence was detected from January to April and in November and December. The observed scintillation activity from March to September/October was not as severe as scintillation activity monitored closer to the magnetic equator (compare Fig. 2). The figure reveals that the main activity was limited from sunset to local midnight, but on occasion continued until dawn. A maximum percentage of 20 to 30 indicates that disturbances occurred in maximum every third to fifth night. A similar picture of the seasonal and diurnal distribution of scintillation occurrence can be expected in every year. Thus, this kind of phase scintillation monitoring helps those GPS user who are interested in highest accuracy to avoid these disturbances.

Example 2: Magnetic Storm April 1993

GPS observations from mid-latitudes sites are usually not affected by ionospheric scintillations. Only in the case of major magnetic storms, small-scale irregularities can penetrate from the polar regions into the mid-latitudes. Several questions arise, for example: How far does the area of ionospheric irregularities extends into the mid-latitudes under storm conditions? Is scintillation occurrence in the polar regions, in the auroral regions, and in the equatorial region correlated with magnetic storms? These questions can be answered with the help of phase scintillation index maps derived from IGS data.

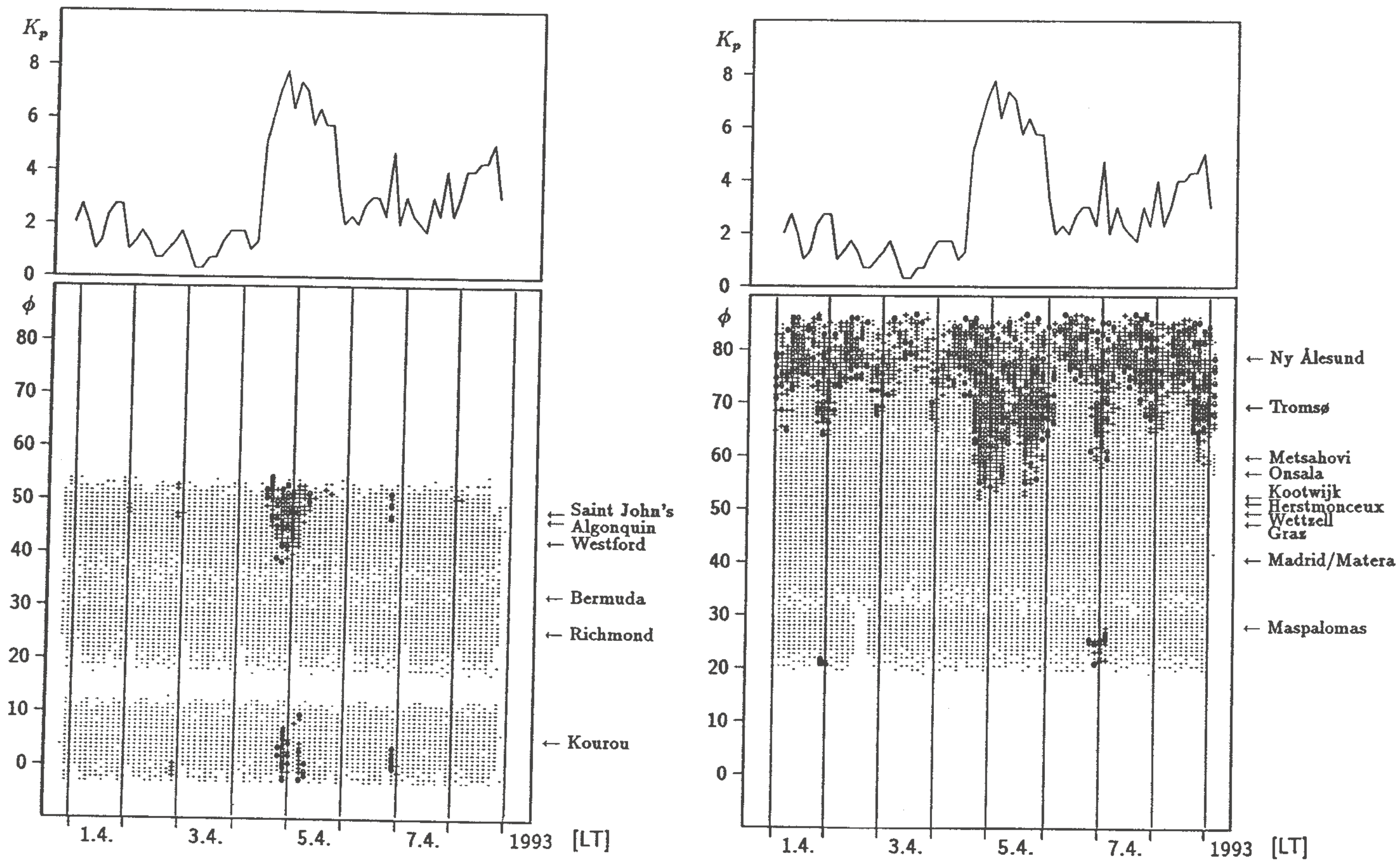

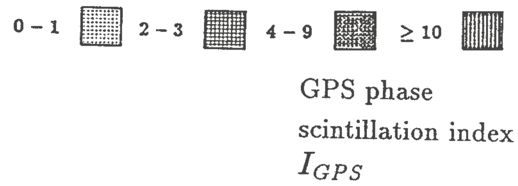

Fig. 6: The development and effects of a major magnetic storm (April 4 and 5, 1993): three-hourly planetary index of geomagnetic activity K_P (upper panels), phase scintillation index I_{GPS} (lower panels) in a coordinate system of local time and geographic latitude (20° elevation mask, 400 km ionospheric height). Fig.6a (left): I_{GPS} from sites at the east coast of the Americas. Fig.6b (right): I_{GPS} from European sites.

An example has been produced for a major magnetic storm which took place on April 4 and 5, 1993. Figures 6a and 6b present the storm effects in the American latitude region and in the European latitude region respectively. The three-hourly planetary index of geomagnetic activity K_P (*SGD 1993*) reveals the development of the storm. It suddenly commenced on April 4, 1993 forenoon local time in America and around noon local time in Europe and and lasted for about 2 days (upper panels in Fig. 6a and 6b). The lower two panels show phase scintillation index maps in a coordinate system of geographic latitude and local time and indicate the latitudes of IGS sites used. The vertical lines mark local midnights. Whereas in the European longitude sector, IGS sites very well cover the latitudes from the polar region (Ny Ålesund) to the northern edge of the equatorial region (Maspalomas), no further sites can be found closer to the center of the equatorial region. At the Atlantic coast of the Americas, the site located furthest north is Saint John's in the northern mid-latitudes. No polar IGS sites exist in this longitude region.

In the European polar region (Ny Ålesund), ionospheric disturbances could be found all day long in the period from April 1 to April 8. Their intensity seems not to be correlated with K_P. In the auroral region (Tromsø), disturbances occurred every night around midnight. During the storm they were very intense and they continuously lasted for about 2 days. In the northern mid-latitudes, no midnight disturbances were detected. But on April 4 and 5, small-scale irregularities extended south to a geographic latitude of 50°. They were not as severe as in the auroral region and they did not occur around noon of April 5. In the northern equatorial region (Maspalomas), disturbances were detected in two night but not during the storm. Their occurrence seems not to be correlated with K_P.

In the American longitude region, the northern mid-latitudes were affected by small-scale irregularities during some nights and especially during the storm. Then, these irregularities extended equatorward to a geographic latitude of less than 40°. In the equatorial region (Kourou), disturbances were detected during three nights with severest effects occurring during the storm. Here, longitudinal differences in scintillation occurrence were found in the equatorial region. Whereas no phase scintillations were detected at Maspalomas on the days of the storm, the GPS observations of Kourou, located at about the same magnetic latitude but 40° further west, were affected.

CONCLUSIONS

Ionospheric scintillations are detectable in GPS signal amplitude observations and GPS phase observations. Since RINEX-formatted observations contain only very little information on the signal amplitude, amplitude scintillations are not detectable in IGS data. The vast amount of IGS continuous dual-frequency GPS phase observations, however, presents an important resource for research on the temporal and geographical occurrence of small-scale ionospheric irregularities. Phase scintillation occurrence maps – as presented in this paper – provide important information for ionospheric research and for users of precise GPS who want to avoid ionospheric disturbances.

REFERENCES

Aarons, J. (1993), The longitudinal morphology of equatorial F-layer irregularities relevant to their occurrence, *Space Science Reviews*, **63**:209-243.

Basu, S., E. MacKenzie, S. Basu (1988), Ionospheric constraints on VHF/UHF communications links during solar maximum and minimum periods, *Radio Science*, **23**:363-378.

Bishop, G., Coco, D.S., Coker, C., Fremouw, E.J., Secan, J.A., Greenspan, R.L., Eyring, D.O. (1992), GPS Application to Global Ionospheric Monitoring: Requirements for a Ground-Based System, in *Proceedings of ION GPS-92*, September 16-18, 1992, Albuquerque, New Mexico, pp.339-353.

Doherty, P.A., Raffi, E., Klobuchar, J.A., El-Arini M.B. (1994), Statistics of Time Rate of Change of Ionospheric Range Delay, in *Proceedings of ION GPS-94*, pp.1589-1598.

Parkinson B.W., Lassiter, E.M., Cretcher, C.K. (1977), Ionospheric Effects in NAVSTAR GPS, in *AGARD Conference Proceedings 209: Propagation Limitations of Navigation and Positioning Systems.*

SGD (1993), *Solar Geophysical Data, Prompt Reports*, No 586-I, June 1993.

UNAVCO (1994), *QC v3 Users Guide*, University NAVSTAR Consortium (UNAVCO), Boulder, March 1994.

Wanninger, L. (1993a), Ionospheric Monitoring using IGS data, in *Proceedings of the 1993 IGS Workshop*, March 25-26, 1993, Bern, Switzerland, pp.351-360.

Wanninger, L. (1993b), Effects of the equatorial ionosphere on GPS, *GPS World*, July 1993, pp.48-54.

Wild, U., Beutler, G., Gurtner, W., Rothacher, M. (1989), Estimating the ionosphere using one or more dual frequency GPS receivers, in *Proceedings of the Fifth International Geodetic Symposium on Satellite Positioning*, Las Cruses, New Mexico, pp.724-736.